NEAR WALL BEHAVIOUR OF STATISTICAL PROPERTIES IN TURBULENT FLOWS

M. Fischer, F. Durst and J. Jovanović
Lehrstuhl für Strömungsmechanik, University of Erlangen-Nürnberg, Cauerstr. 4
91058 Erlangen, Germany

ABSTRACT

The continuity and momentum equations do not imply a Reynolds number dependence of turbulence data when wall variables are used for normalization. The influence of the Reynolds number on turbulence quantities results from the imposed boundary conditions at the edge of a boundary layer or on the axis of a channel or a pipe flow. This has often been assumed not to affect the near wall region. However, experimental and numerical results show a Reynolds number dependence of turbulence intensity very close to the wall. It results from the behaviour of a sink term in the dissipation rate equation which shows a Reynolds number dependence in the limit of two-component two-dimensional turbulence as it exists close to walls. Away from the near-wall region the Reynolds number dependence originates from the streamwise pressure gradient which enters into the equations for the turbulent kinetic energy and turbulent dissipation rate through the gradient production processes. The low-Reynolds number effects in turbulent channel flow were investigated experimentally using the LDA measuring technique. A new method was applied to eliminate the influence of the limited spatial resolution of the measuring technique.

INTRODUCTION

Fully developed turbulent pipe and channel flows are subclasses of wall-bounded flows that have been extensively investigated in the past. Although we have collected an impressive body of experimental data over past 50 years, the overall progress achieved in the field is slow. In part this is due to the lack of the appropriate data which could be used to analyze the complete dynamic equations for the turbulence correlations. With advances in computer technology it has become feasible to study turbulent flows by applying numerical techniques. While there is a general agreement in the literature about scaling of the mean velocity distribution close to the wall, there is no physical explanation for important variations of the fluctuating quantities when non-dimensionalized using the wall variables.

The goal of this paper is to investigate the influence of the Reynolds number in the near-wall region of fully developed channel flows. We will focus our attention primarily on the region of viscous sublayer adjacent to the wall where it is expected that inner scaling laws should hold by definition for all turbulence quantities.

In the region very close to the wall high gradients exist and the questions regarding the data accuracy and the spatial resolution are most serve for experimental *and* numerical investigations.

The laser-Doppler (LDA) measuring technique allows accurate experimental data to be obtained deep in the viscous sublayer provided that the influence of the finite size of the LDA control volume is taken into account. Turbulence quantities, measured by LDA, show dependence on the measuring volume size and require application of the volume corrections which can be derived analytically. By measuring with different LDA volume sizes the high reliability of the turbulence data can be achived close to the wall even at high Reynolds numbers.

ANALYSIS OF DNS DATA

ENERGY BALANCE

In this section we shall utilize the numerical databases to examine the influence of Reynolds number on the terms in the budget for the turbulent kinetic energy $k = 1/2\overline{u_s u_s}$:

$$\frac{\partial k}{\partial t} + \overline{U}_k \frac{\partial k}{\partial x_k} = \underbrace{-\overline{u_i u_k}\frac{\partial \overline{U}_i}{\partial x_k}}_{P_k} \underbrace{-\frac{1}{2}\frac{\partial}{\partial x_k}\overline{u_s u_s u_k}}_{T_k}$$
$$\underbrace{-\frac{1}{\rho}\frac{\partial}{\partial x_i}\overline{pu_i}}_{\Pi_k} \underbrace{-\nu\overline{\frac{\partial u_i}{\partial x_k}\frac{\partial u_i}{\partial x_k}}}_{\epsilon} + \underbrace{\nu\frac{\partial^2 k}{\partial x_k \partial x_k}}_{D_k}. \quad (1)$$

Since in the channel flow convection is negligible, the balance of (1) consists of production (P_k), turbulent (T_k) and pressure (Π_k) transport, dissipation (ϵ) and viscous diffusion (D_k). This is indicated in figure 1, where we plotted the individual terms which contribute to the balance of the k equation for five different Reynolds numbers, Re_m=2900, 4600, 5600, 6700 and 13800, based on the bulk velocity ($\overline{U}_m$) and full width (H=2h) of the channel. For this purpose databases of Kim *et al.* (1987), Kuroda *et al.* (1989, 1993), Horiuhi (1992), Gilbert & Kleiser (1991) and Antonia *et al.* (1992) were employed. The viscous diffusion (D_k) is also sensitive to variations in Re but plays passive role and serves only to satisfy the boundary conditions at the wall. The turbulent (T_k) and pressure (Π_k) transport are relatively insensitive to the Reynolds number dependence.

Using the mean momentum equation

$$1 - \frac{x_2^+}{Re_\tau} = \frac{d\overline{U}_1^+}{dx_2^+} - \overline{u_1^+ u_2^+},$$

the production rate term in (1) may be expressed as follows:

$$P_k^+ = \frac{d\overline{U}_1^+}{dx_2^+} - \frac{x_2^+}{Re_\tau}\frac{d\overline{U}_1^+}{dx_2^+} - \left(\frac{d\overline{U}_1^+}{dx_2^+}\right)^2, \quad (2)$$

where Re_τ is the Reynolds number $Re_\tau = u_\tau h/\nu$ based on the half-width (h) of the channel. The second term on the right- hand side of (2) originates from the streamwise pressure gradient, which can be determined from the shear stress at the wall. As can be inferred from (2), the production term exhibits a strong Reynolds number dependence even very close to the wall.

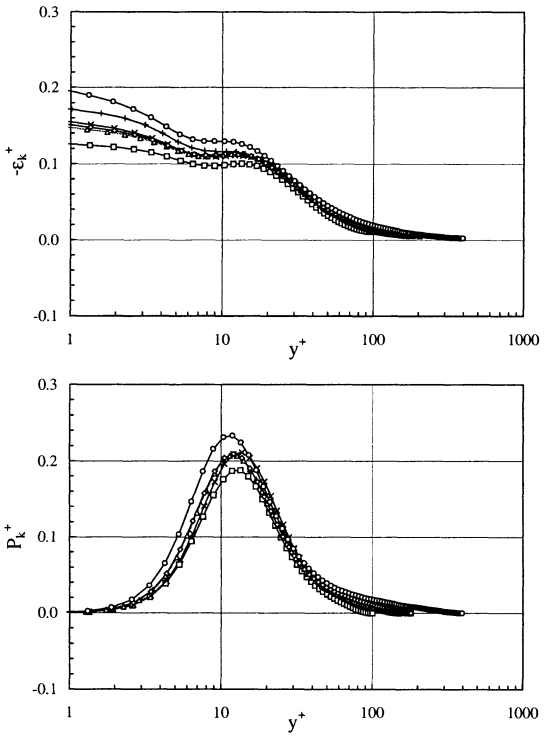

Figure 1: Balance of the turbulent kinetic energy in a plane channel flow for different Reynolds numbers.

Based on these results, one may conclude that the source of the observed low Reynolds number effects in a boundary layer lies in the dissipation equation. Further analysis of the Reynolds number dependence of the turbulent dissipation rate requires the introduction and application of the anisotropy invariant theory as changes in the Reynolds number may be reflected in a change of the anisotropy.

ANISOTROPY INVARIANT MAPPING

The anisotropy of the turbulence can be quantified, according to Lumley & Newmann (1977), using the anisotropy tensor

$$a_{ij} = \frac{\overline{u_i u_j}}{q^2} - \frac{1}{3}\delta_{ij},$$

and its scalar invariants:

$$II_a = a_{ij}a_{ji},$$
$$III_a = a_{ij}a_{ik}a_{jk}.$$

A plot of (13) versus (14) for axisymmetric turbu-

lence:

$$II_a = \frac{3}{2}\left(\frac{4}{3}|III_a|\right)^{2/3},$$

and two-component turbulence:

$$II_a = \frac{2}{9} + 2III_a,$$

defines the anisotropy invariant map, which according to Lumley (1978) bounds all physically realizable turbulence. It is interesting to analyze the influence of Reynolds number on the anisotropy of the Reynolds stresses since it can shed some light on the dynamics of turbulence in the near-wall region. Figure 2 shows the effect of Reynolds number on the anisotropy of the turbulence for channel flow. There are two noticeable trends in the data that can be clearly distinguished:

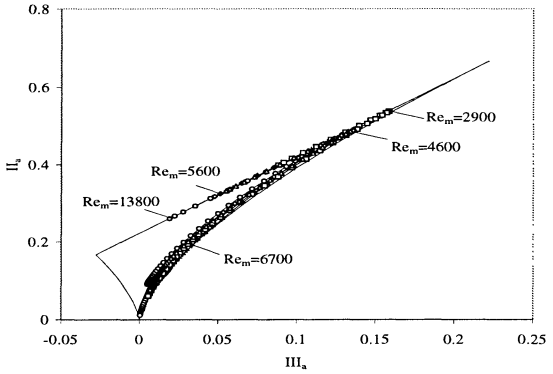

Figure 2: Traces of the joint variations of II_a and III_a across the anisotropy invariant map. Data correspond to a plane channel flow at different Reynolds numbers.

(i) With increasing the Reynolds number the anisotropy very close to the wall decreases. Consequently, the invariants, which are lying along the two-component limit, tend to move towards the left corner point of the anisotropy map, which corresponds to the two-component isotropic state.
(ii) In the buffer and logarithmic flow regions the invariants closely follow the right boundary of the anisotopy map, which corresponds to axisymmetric turbulence. From figure 2 it appears that with increase in Reynolds number there is a trend in the data to shift gently towards the limit valid for two-component turbulence.

We may try to use the above-mentioned inferences gained from the numerical databases in order to explain the observed low Reynolds number effects close to the wall which are concentrated in the dynamic equation for the turbulent dissipation rate. This is plausible since the dynamics of ϵ are influenced by the anisotropy of the turbulence. We shall see later how the Reynolds number dependence of ϵ at the wall actually arises.

DISSIPATION RATE BALANCE

In the studies of Jovanović *et al.* (1995,1996), the two-point correlation technique and the invariant theory were used to examine turbulence closure for dissipation rate correlations. The results of the analysis were found to be consistent with the suggestion made by Lumley (1978) that the anisotropy of turbulence plays an important role in the budget of dissipation rate correlations. Based on these considerations Jovanović *et al.* (1995,1996) derived the following set of the equations which govern approximately the dynamics of the turbulent dissipation rate:

$$\epsilon = \frac{1}{2}\nu\Delta_x k + \epsilon_h, \tag{3}$$

$$\frac{\partial \epsilon_h}{\partial t} + \overline{U}_k\frac{\partial \epsilon_h}{\partial x_k} = -2A\,\frac{\epsilon_h \overline{u_k u_s}}{k}\,\frac{\partial \overline{U}_s}{\partial x_k} - \psi\frac{\epsilon_h^2}{k} + \frac{\partial}{\partial x_k}\left(C_\epsilon \frac{k}{\epsilon_h}\overline{u_k u_l}\frac{\partial \epsilon_h}{\partial x_l}\right) + \frac{1}{2}\,\nu\Delta_x\epsilon_h. \tag{4}$$

According to (3), the turbulent dissipation rate ϵ is composed of an inhomogeneous $1/2\nu\Delta_x k$ part and a homogeneous part ϵ_h. The homogeneous part of the dissipation rate ϵ_h is directly related to the Taylor microscale λ as $\epsilon_h = 5\nu q^2/\lambda^2$.

The first two terms on the right-hand side of (4) approximate the production of ϵ_h by the mean velocity gradient. Examination of the limiting behaviour of the two-point velocity correlation for the various states of turbulence permitted the closure for the generation of ϵ_h to be expressed in terms of the anisotropy of turbulence and turbulent Reynolds number:

$$-2A\frac{\epsilon_h}{k}\overline{u_k u_l}\frac{\partial \overline{U}_k}{\partial x_l}, A = A(II_a, III_a, R_\lambda), R_\lambda = \frac{\lambda q}{\nu}.$$

In two-component turbulence and for arbitrary Reynolds number, the invariant function A has the value $A = 1$. For vanishing anisotropy and very low Reynolds numbers, $A = 1$. For small anisotropy and very large Reynolds numbers $A \simeq 0$, which is in close agreement with the Kolmogorov's (1941) theory of locally isotropic turbulence.

The third term on the right-hand side of (4) is

$$-\psi\frac{\epsilon_h^2}{k}, \quad \psi = \psi(II_a, III_a, R_\lambda),$$

an approximation of the difference between the turbulent production and viscous destruction the two dominant terms in the balance of the dissipation rate equation.

The fourth term on the right-hand side of (4) accounts for the turbulent transport. The most widely used closure for this term

$$\frac{\partial}{\partial x_k}(C_\epsilon \frac{k}{\epsilon_h}\overline{u_k u_l}\frac{\partial \epsilon_h}{\partial x_l}), \quad C_\epsilon \simeq 0.18, \tag{5}$$

is analogous to the form used for the interpretation of the similar term in the energy equation. Using the scaling arguments outlined by Tennekes & Lumley (1972), Jovanović *et al.* (1996) derived the alternative closure:

$$-\frac{7\sqrt{3}}{180}\frac{\partial}{\partial x_k} J f_\epsilon \frac{\epsilon_h}{k}\overline{q^2 u_k}, \; J = J(II_a, III_a), f_\epsilon = f_\epsilon(R_\lambda). \tag{6}$$

In contrast to (5), the use of (6) permits a nearly perfect balance of the dissipation rate equation to be obtained from the experimental data measured near the centreline of a plane turbulent wake flow at low Reynolds number.

The last term on the right-hand side of (4) is the viscous diffusion of ϵ_h.

The asymptotic values of the invariant functions A, ψ and J at three corner points of the anisotropy invariant map can be matched together using the invariant theory. Based on the these considerations, the reformulated closure of the dissipation rate equation given by (3) and (4) can cover the entire anisotropy invariant map, i.e. all physically realizable turbulence.

We may now examine the closure of the ϵ_h equation (4) with the aim of isolating the cause of the previously described Reynolds number variation of ϵ near the wall. In the region of viscous sublayer, the decay term $(-\psi\epsilon_h^2/k)$ of the dissipation rate equation is balanced by the viscous diffusion term $(1/2\nu\Delta_x\epsilon_h)$. For this reason, only an increase in ψ can raise the viscous diffusion and also ϵ at the wall. However, the trend in the data extracted from numerical simulations indicates that the anisotropy of turbulence at the wall decreases with increasing Reynolds number. This trend implies a decrease in ψ and ϵ at the wall with increasing Reynolds number.

However, the above consideration does not account for the effects of the dimensionality of turbulence close to the wall. As the wall is approached the normal velocity component vanishes much faster than other two components and the flow is forced to move in the planes which are parallel to the wall. Thus, to a first approximation, turbulence in the viscous sublayer might be considered as two-component and two-dimensional. For such a state ψ may be approximated in the form $\psi_{2C-2D} \simeq 0.02R_\lambda$. This form eliminates singularity in the sink term of the dissipation equation when it is applied to the flow predictions close to the wall. Therefore, we may conclude that *the behaviour of* $(\psi)_{2D-2C}$ *very close to the wall is responsible for rise in* ϵ *at the wall with increasing Reynolds number.*

EXPERIMENTAL INVESTIGATIONS

From the analysis carried out in Section 2 the reader may come to the conclusion that the numerical databases form a firm basis for investigating the dynamics of turbulence in a channel flow and that there is no need for the additional experimental data in order to clarify the low Reynolds number effects close to the wall. However, examination of the budget of the dissipation rate equation close to the wall reveals noticable discrapencies between the numerical databases in the near-wall region.

From this arises the question how much of the observed Reynolds number variation is due to physical effects and how much is based on numerical uncertainties. For the above reason, it is desirable to perform additionally measurements under well-controlled laboratory conditions and at similar Reynolds numbers as these deliver flow information which is independent of numerical limitations.

To study the low Reynolds number effects in fully developed plane channel flows, a water flow facility was set up which permitted mean velocities of up to 2.5 m/s to be obtained. The channel test section of dimensions $l \times b \times H = 1 \times 0.18 \times 0.01$ m was preceded by a rectangular contraction chamber (0.15×0.18 m). The measurements were performed 71 channel heights downstream of the inlet using a laser-Doppler anemometer.

Two different LDA systems were used in the present study in order to ensure good spatial and temporal resolution of the measurements.

LDA CONTROL VOLUME EFFECTS

Owing to the spatial distribution of turbulent fluctuations, the Doppler shift frequency obtained from each scattering particle does not correspond to the velocity in the centre of the measuring control volume but represents the time and volume integrated information. In Durst *et al.* (1998) equations for the correction of control volume effects

statistical properties are derived. The ellipsoidal shape of the control volume and the constant size of the scattering particles were taken into account. Taylor series expansion of the mean and the fluctuating parts of the velocity and spatio-temporal integration delivers the expressions for the measured mean velocity and turbulent intensity:

$$\overline{U}^+_{i,c_v} \approx \overline{U}^+_{i,c} + \frac{d_2^{+2}}{32}\left(\frac{\partial^2 \overline{U}_i^+}{\partial x_2^{+2}}\right)_c ,$$

$$\overline{u^{+2}_{i,c_v}} \approx \overline{u^{+2}_{i,c}} + \frac{d_2^{+2}}{32}\left[2\left(\frac{\partial \overline{U}_i^+}{\partial x_2^+}\right)_c^2 + \left(\frac{\partial^2 \overline{u_i^{+2}}}{\partial x_2^{+2}}\right)_c\right]$$

The measured mean velocity turnes out to be very close to the time-averaged value at the centre of the measuring control volume as the second derivative of the mean velocity profile is negligible in close proximity to the wall. The correction for the turbulent intensity is proportional to the mean velocity gradient and to the curvature of the intensity profile near the wall. The sum of both correction terms enlarges the measured intensity in comparison with the value at the centre of the measuring control volume. Detailed analysis shows that measured turbulent intensities can be increased at more than 100% (Durst *et al.*, 1998).

The reliability of the computed values of turbulent fluctuations depends on the accuracy of the control volume diameter. As the detection of the bursts is influenced by the size of the scattering particles, the transmitting and receiving optical system and the electronical settings of the signal processing electronics, the effective size of the control volume is not unique. Therefore preceding measurements in laminar flows were undertaken in order to calibrate the effective control volume size d_2. For such flows (7) deliveres a direct proportionality between the relative mean velocity gradient and the measured effective turbulence level:

$$\underbrace{\sqrt{\frac{u'^2_{1,c_v}}{\overline{U}_1^2} - \frac{u'^2_{\text{noise, optics}}}{\overline{U}_1^2}}}_{\text{effective turbulence level}} = d_2 \cdot \underbrace{\frac{1}{4\overline{U}_1}\left(\frac{\partial \overline{U}_1}{\partial x_2}\right)_c}_{\text{relative mean velocity gradient}} .$$

EXPERIMENTAL RESULTS

In Fig. 3 the mean velocity distributions for various Reynolds numbers are shown. A systematic

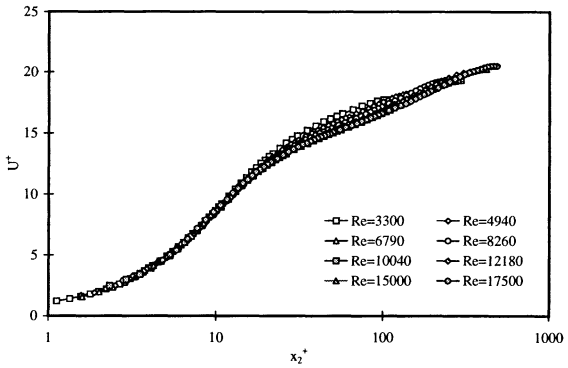

Figure 3: Mean velocity profiles non-dimensionalized on inner variables

variation in the core region of the flow with increasing Reynolds number can be reported. Of particular interest was the behaviour very close to the wall. Analysis of data from DNS have shown that at the outer edge of the viscous sublayer, the sum of the pressure drop term and the Reynolds stress term are nearly independent of Reynolds number and therefore cannot be resolved experimentally. According to direct numerical simulations of turbulent channel flow, the streamwise velocity component accounts for about 75% of the dissipation rate at the wall (Kim et al., 1987; Antonia et al., 1992): $(\epsilon^+)_{Wall} \approx 1.3\left(\frac{u'^2}{U^{+2}}\right)_{Wall}$. Therefore the measurement of streamwise turbulent fluctuations gives an insight into the influence of Reynolds number on $(\epsilon^+)_{wall}$. In Fig. 4 the RMS-values of the

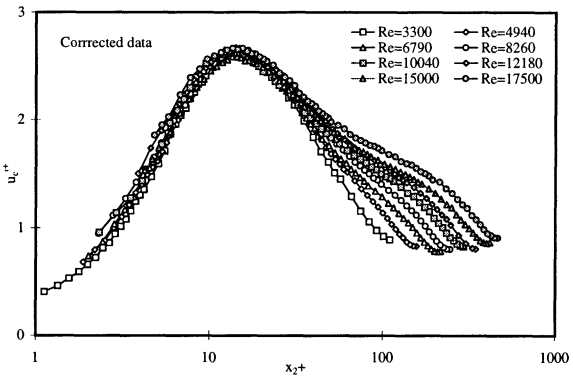

Figure 4: Profiles of the RMS values of turbulent fluctuation measured (top) and corrected (bottom)

corrected data are shown. For the evaluation of the wall limiting values of the turbulence level, the near wall data in the region $y^+ < 10$ were extrapolated to the wall position. In Fig. 5 the resulting

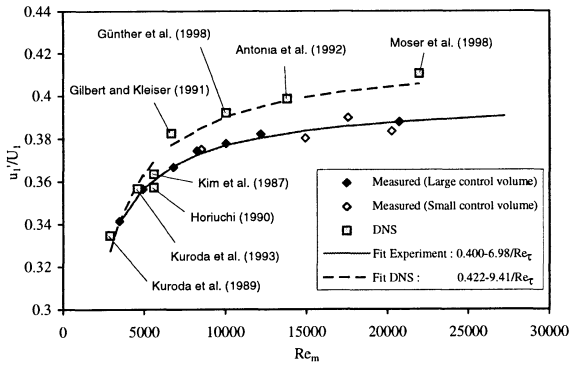

Figure 5: Plot of determined wall limiting values for u'/U. Comparison with DNS-data

values extracted from the measurements are plotted against Reynolds number. Comparison between experiment and DNS results reveals the same trend but a remarkable deviation in the absolute values of u'/U at higher Reynolds numbers. The measured turbulent fluctuations can be approximated quite well by an analytical expression that contains a limiting value for very high Reynolds numbers and a subtractive part inversely proportional to the Reynolds number.

$$(u'/U)_{Wall} = (u'/U)_{Wall;Re\to\infty} - A/Re_\tau \qquad (7)$$

Fitting of Eq. (7) yields for the constants: $(u'/U)_{Wall;Re\to\infty} = 0.40 \pm 0.01$ $A = 7.0 \pm 0.5$. Extrapolating this result, one would expect the Reynolds number effects to vanish asymptotically above $Re_m \approx 35000$.

CONCLUSIONS

The previous sections have delivered both analytical results supported by numerical data and experimental results in the Reynolds number range between 3,000 and 25,000. Both of these data sets reveal similar trends with increasing Reynolds number. The wall limit of $u_1'/\overline{U}_1$ high Reynolds numbers turns out to be 0.4. This value can be used as a criterion turbulence models at the wall have to fulfil. Statistical analysis carried out in Section 2 shows that the decay term of the dissipation rate equation is responsible for the low Reynolds number effects.

Away from the very near-wall region the Reynolds number dependence of the turbulence statistics is caused by the streamwise pressure gradient which contribute to the production processes in the equations for the turbulent kinetic energy and turbulent dissipation rate. Anisotropy invariant mapping of the Reynolds stress tensor reveals the tendency in the turbulence statistics to shift slightly from nearly axisymmetric state towards the two-component state. This trend implies a gentle increase of the turbulent dissipation rate in the buffer and logarithmic flow regions with increasing the Reynolds number. Joint application of analytical and experimental methods has resulted in a valuation of numerical data bases and in an improved insight into the mechanisms of Reynolds number effects on turbulent fluctuations near rigid walls.

REFERENCES

Durst, F.; Kikura,H.; Lekakis, I.; Jovanović, J.; Ye, Q.-Y., 1996, "Wall shear stress determination from near-wall mean velocity data in turbulent pipe and channel flows", *Exp. Fluids* 67: 257-271

Durst, F.; Fischer, M.; Jovanović, J.; Kikura, H., 1998, "Methods to set up and investigate low Reynols number, fully developed turbulent plane channel flows", *J. Fluid Eng.* 120: 496-503

Gilbert, N. and Kleiser, L., 1991, "Turbulence model testing with the aid of direct numerical simulation results", *8th Symp. on Turbulent Shear Flows*, Sept. 9-11, TU Munich, pp. 26.1.1-26.1.6

Jovanović, J.; Ye, Q.-Y. and Durst, F., 1995, "Statistical interpretation of the turbulent dissipation rate in wall-bounded flows", *J. Fluid Mech.* 293: 321-347

Jovanović, J.; Ye, Q.-Y.; Jakirlić, S. and Durst, F., 1996, "Turbulence closure for dissipation rate correlations", submitted to *J. Fluid Mech.*

Kim, J.; Moin, P. and Moser, R., "Turbulence statistics in fully developed channel flow at low Reynolds number", *J. Fluid Mech.* 177: 133-166, 1987

Kim, J., 1990, "Collaborative Testing of Turbulence Models (Organized by P. Bradshaw)", Data Disk No.4.

Kuroda, A.; Kasagi, N. and Hirata, M., 1989, "A direct numerical simulation of fully developed turbulent channel flow", *Int. Symp. on Comput. Fluid Dynamics*, Nagoya, pp 1174-1179

Kuroda, A.; Kasagi, N. and Hirata, M., 1993, "Direct numerical simulation of the turbulent plane Couette-Poiseulle flows: Effect of mean shear on the near wall turbulence structures", *9th Symp. on Turbulent Shear Flows*, Kyoto, Japan, Aug. 16-18, pp. 8.4.1-8.4.6